Journal of Electroceramics 2:2, 75–84, 1998

Detailed X-ray Diffraction Analyses and Correlation of Microstructural and Electromechanical Properties of La-doped PZT Ceramics

MARIANNE HAMMER & MICHAEL J. HOFFMANN
University of Karlsruhe, Institute of Ceramics in Mechanical Engineering, Haid-und-Neu-Str. 7; D-76131 Karlsruhe, Germany

Submitted August 22, 1997; Revised March 5, 1998; Accepted March 17, 1998

Abstract. The influence of the La-concentration (0.1– 8 mole-%) on the F_R/F_T-ratio and the c/a-ratio of mixed oxide derived stoichiometric and 3 mole-% PbO excess containing PZT with a Zr/Ti-ratio near the morphotropic phase boundary (53/47) was investigated by quantitative X-ray diffraction analysis. Temperature dependent X-ray diffraction measurements showed a decrease of the Curie-temperature for La-additions > 0.5 mole-% but an increase for very low La-amounts (0.1 and 0.2 mole-%) in comparison to undoped samples. Obviously this phenomenon indicates the influence of La-dopants on the vacancy concentration and thereby on the stability of the crystal structure. The change in vacancy concentration leads to a different densification behavior for undoped and doped samples which could be shown by dilatometric measurements. The observations were finally correlated to measurements of dielectric constants and coupling factors which additionally show a strong dependence on the PbO excess and the microstructure (porosities, grain sizes and chemical inhomogeneities) of PZT ceramics.

Keywords: quantitative X-ray diffraction analysis, F_R/F_T-ratio, c/a-ratio, Curie-temperature, La-doping, microstructural and electromechanical properties

1. Introduction

Cooling a PZT solid solution with a composition near the morphotropic phase boundary (MPB) below its Curie-temperature (T_C) induces a phase transformation from the paraelectric cubic (P_C) to the ferroelectric rhombohedral (F_R) and ferroelectric tetragonal (F_T) PZT modification [1]. Simultaneously with the transformation occurs a distortion of the unit cells which is of different cristallographic directions for the F_T- ($\{001\}$-direction) and for the F_R-phase ($\{111\}$-direction) [2,3]. For undoped F_T PZT (45/55) Endriss [3] measured by means of Bragg-Brentano X-ray diffraction a c/a-ratio of 1.0332(1) whereas the F_R-modification (60/40) showed a $d_{111}/d_{11\bar{1}}$ ratio of only 1.007. However, for an undoped morphotropic composition with a Zr/Ti-ratio of 53/47 the c/a- ratio of the F_T-modification decreases to 1.023 [4] and the typical strong overlapping of the $F_{T(200)}$-, $F_{T(002)}$- and $F_{R(200)}$-peaks in the range of $43° \leq 2\Theta \leq 46°$ could be observed. Furthermore, donor and acceptor doped PZT ceramics (La, Nd, Nb, Ta, Ag) show a decrease of the c/a-ratio and the Curie-temperature (T_C) [1,2,4,5]. For soft PZT, Thomann [6], and Heywang and Schöfer [7] attribute this effect to the formation of Pb-vacancies which are created in order to obey the electroneutrality condition in the perovskite lattice. The Pb-vacancies partially disturb the coupling of Ti(*Zr*)—O-chains and the more covalent bonded Pb—O-coordination polyhedra. Due to this fact, donor doping lowers the c/a-ratio which consequently results in a decrease of the spontaneous polarization (P_s) and the Curie-temperature (T_C). In addition, Thomann [6] and Wersing et al. [8] stated that there is a continuous increase of piezoelectricity in the tetragonal phase from pure $PbTiO_3$ towards the phase boundary which is accompanied by an increase of dielectric permittivity. This holds not only for ε_{33} measured parallel to the piezoelectric axis, but also for

ε_{11} measured perpendicular to the axis. Wersing et al. [8] has shown that the microscopic permittivity ε^*_{33}, i.e., parallel to the spontaneous polarization within a single domain, is significantly smaller than the microscopic permittivity ε^*_{11} and depends on composition. As the measured macroscopic permittivity ε_{33} can be calculated as a mixture of the microscopic ones the permittivity ε_{33} is dominated by ε^*_{11}. The authors [6,8] explain this behavior in terms of stereochemistry. In $PbTiO_3$ only one of the three rectangular Ti—O-chain systems is polarized, whereas the other ones are kinked. With increased substitution of Zr for Ti, the tetragonal lattice distortion becomes smaller. The perpendicular Ti—O-chains are less kinked and consequently they are more polarizable developing a higher polarizability and permittivity ε^*_{11}. Beside the Zr/Ti-content the dopant concentration strongly influence the c/a-ratio which additionally alter the polarizability. However, not only the unit cell distortion is of importance for the resulting polarizability but also the domain wall mobility which differs strongly in soft and hard PZT ceramics.

It is known that donor-doped PZT ceramics with a morphotropic composition reveal the best dielectric properties [9–12] and most of the investigations were done in the system PbO-ZrO_2-TiO_2-La_2O_3 (Nd_2O_3) [9,12–14]. For example an addition of La stabilizes the F_T-phase [10,12,13] which strongly influences the electromechanical properties (ε and k_p) [2,12–14]. However, former investigations in La- and Nd-doped PZT systems showed that an addition of very low dopant concentrations (<0.5 mole-%) lead to high porosities and therefore to low and unreproducible electromechanical properties [12,14]. Consequently, in terms of application, those compositions were not of interest and no further investigations have been performed.

The purpose of this paper is not an optimization of PZT-ceramics with different Zr/Ti-ratios and La-contents, but a detailed quantitative X-ray diffraction analysis of the F_R/F_T-ratio, the c/a-ratio and the T_C in La-doped (0.1–8 mole-%) stoichiometric and 3 mole-% PbO-excess containing PZT ceramics, in order to study the influence of the composition on the microstructural development (porosity, grain size and chemical homogeneity) and the related electromechanical properties. Although it is well known that the MPB shifts with an increasing La-content, the Zr/Ti-ratio was kept constant at 53/47. Nevertheless, the shift of the MPB could be indirectly studied by measuring the F_R/F_T-ratio of the corresponding samples.

2. Experimental Procedure

Stoichiometric and 3 mole-% PbO excess containing PZT samples ($Pb_{1-3x}La_{2x}(Zr_{1-y}Ti_y)O_3$) with different Zr/Ti-ratios and La-concentrations ($0.001 \leq \times \leq 0.08$) were prepared by the conventional mixed oxide process. The La-ions were supposed to substitute only A-site ions. The oxides (PbO,[1] ZrO_2,[2] TiO_2[3] and La_2O_3[4]) were homogenized for 3 h by attrition milling using ZrO_2 balls and isopropanol as milling media. After drying in a rotation evaporator, the powder mixtures were calcined in air at 850°C for 2 h. The as-received PZT solid solutions were subsequently treated in isopropanol for 4 h in a ball mill to break up the agglomerates. The dried and sieved powders were afterwards consolidated into green compacts of 15 mm thickness and 10 mm diameter by using rubber moulds and cold isostatic pressing at 630 MPa. Sintering was performed in an oxygen atmosphere in a $PbZrO_3 + 8$ wt.-% ZrO_2-powder bed in order to establish a constant PbO vapor pressure during densification [15]. The sintering temperature was 1200°C and the isothermal sintering time was kept constant for 2 h.

X-ray analysis were performed using a D5000, Fa. Siemens with Bragg-Brentano geometry, Cu-$K_{\alpha 1}$-radiation and a goniometer speed of 0.02°/20 s in order to calculate the F_T- and F_R-content, the volume of the unit cells (V_{UC}) and the c/a-ratios of the sintered samples. The measuring time gives counting rates (n) of approximately 3000 C/20 s resulting in an average error of $R < 1.8\%$:

$$R[\%] = \frac{1}{\sqrt{n_{Reflex}}} \cdot 100 \tag{1}$$

The F_T- and F_R-contents were quantified by the intensities of the overlapping $F_{T(200)}$-, $F_{T(002)}$- and $F_{R(200)}$-peaks in the angle range of $43 \leq 2\Theta \leq 46°$ using least square refinement with Lorentzian profile functions. For the determination of the F_R-phase content the following equation was used:

$$x_{F_R} = \frac{I^{Int}_{F_{R(200)}}}{I^{Int}_{F_{T(200)}} + I^{Int}_{F_{T(002)}} + I^{Int}_{F_{R(200)}}} \tag{2}$$

Curie-temperature measurements were performed in the temperature range of 30–400°C with a Guinier diffractometer [16,17] (Cu-K_α, 45 kV and 80 mV). In order to avoid any surface texture effects [5,18,19] all measurements were done on sintered, powderized and heat treated (500°C/4 h) solid solutions.

The electrical properties were investigated on poled and unpoled discs with a diameter of 8 mm and a thickness of 0.5 mm. The poling was performed at 150°C and 3 kV/mm in SF_6 gas. Dielectric constant and coupling factor measurements were carried out with a Wayne-Kerr B905 bridge and a HP 4195A, respectively. The microstructures were studied by a scanning electron microscope (Stereoscan 200, Cambridge Instruments, England) of polished and etched surfaces. The grain sizes and relative densities were determined by quantitative image analysis.

3. Results

3.1. Densification Behavior

Figure 1 shows the relative density, determined by quantitative image analysis, as a function of the additive content. Samples containing low La additions (0.1 and 0.2 mole-%) reveal a higher porosity (12.6% and 11.7%, respectively) than the undoped or ≥ 0.5 mole-% La-containing ones. However, a comparison of stoichiometric and PbO excess containing samples clearly shows a higher densification for stoichiometric compositions (Fig. 1). In general the densities of stoichiometric samples with ≥ 0.5 mole-% La-content are $> 98.5\%$ and slightly lower for La-concentrations > 4 mole-% (approximately 97.5%). The additive dependency of the grain size shows the inverse tendency of the relative density plot (Fig. 2). The grain size reveals a maximum for stoichiometric samples with 0.2 mole-% La-additions (9.25 μm). An increase of La-content up to 3 mole-% leads to a continuous decrease in grain sizes independent of the PbO-content (0.91 μm for stoichiometric compositions and 0.80 μm for samples with PbO excess) but no further significant difference could be observed for higher dopant concentrations (Fig. 2).

3.2. X-ray Diffraction Analyses and Microstructure

X-ray diffraction patterns of undoped PZT with different Zr/Ti-ratios are shown in Fig. 3. Compositions with a high Zr-content (60 mole-%) and a low Zr-content (45 mole-%) show a single phase rhombohedral (F_R) and tetragonal (F_T) solid solution, respectively. To find the optimal morphotropic composition which is approximately at a F_R/F_T-ratio of 50/50, PZT solid solutions with Zr/Ti- ratios $0.52 \leq Zr_x \leq 0.55$ were prepared (Fig. 3). The F_R/F_T-ratios were calculated by least square refinement with Lorentzian profile functions of the overlapping $F_{T(200)}$-, $F_{T(002)}$- and $F_{R(200)}$-peaks. Figure 4 shows as an example the refinement of each peak intensity and the corresponding sum of the Lorentzian curves. Obviously the sum of the curves fits well with the experimental data and the Zr/Ti-ratio for an optimal morphotropic composition was determined at 53/47.

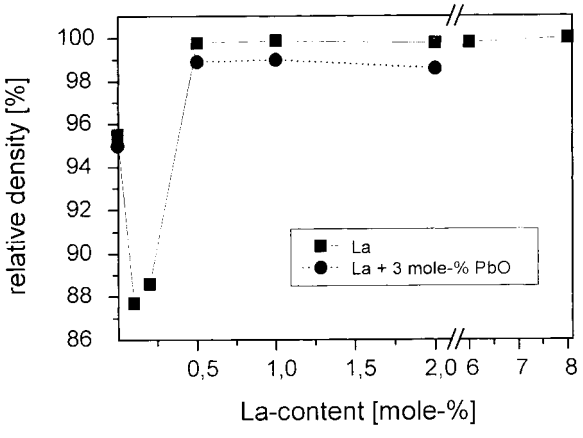

Fig. 1. Influence of La-content on the relative density.

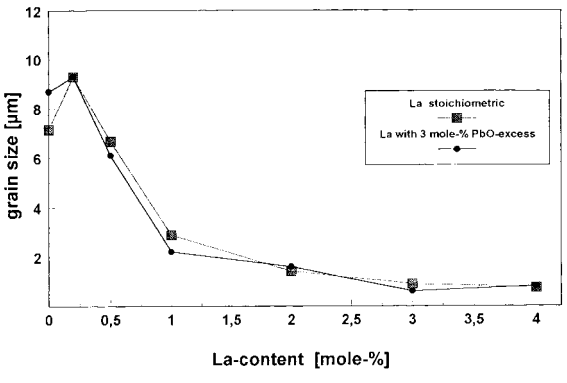

Fig. 2. Influence of La-content on the grain size.

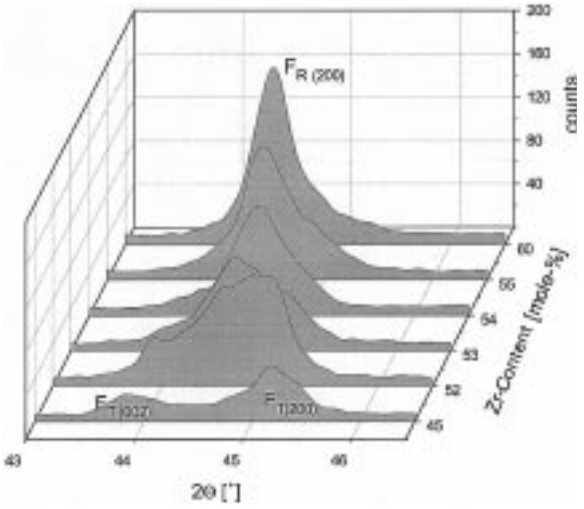

Fig. 3. X-ray diffraction patterns of undoped PZT solid solutions with different Zr/Ti-ratios.

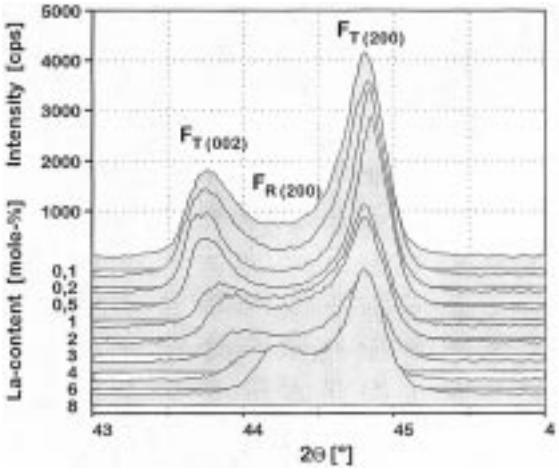

Fig. 5. X-ray diffraction patterns of stoichiometric PZT solid solutions with a Zr/Ti-ratio of 53/47 and different La-concentrations.

PZT solid solutions with a fixed Zr/Ti-ratio of 53/47 and different amounts of La $(0.001 \leq \times \leq 0.08)$ were prepared to analyze the influence of donor doping on the shift of the morphotropic phase boundary. The corresponding X-ray diffraction patterns in the angle range of $43° \leq 2\Theta \leq 46°$ with the typical overlapping of the $F_{T(200)}$-, $F_{T(002)}$- and $F_{R(200)}$-peaks are shown in Fig. 5. The patterns clearly show that an increase of La leads to a change of the F_R/F_T-ratio. A quantification of the F_R/F_T-ratios was achieved by using the experimental peak intensities and the peak refinement already described for undoped samples. The calculated F_T-phase content is illustrated in Fig. 6. In comparison to the undoped PZT solid solution all La-doped samples reveal a higher F_T-phase content. However, no continuous increase of the F_T-phase could be observed with increasing additive content. For samples with low La-concentrations (0.1 and 0.2 mole-%) the F_T-content is higher than for La-additions of 0.5 to 3 mole-%. The F_T-content increases again for additive contents > 3 mole-%.

Additionally the lattice parameters of the $F_{T(200)}$-, $F_{T(002)}$- and $F_{R(200)}$-peaks were determined on basis of the refined data. For the F_T-phase the resulting c/a-ratios and the corresponding volume of the unit cells V_{uc} are shown in Fig. 7 and Table 1. The V_{uc} for the

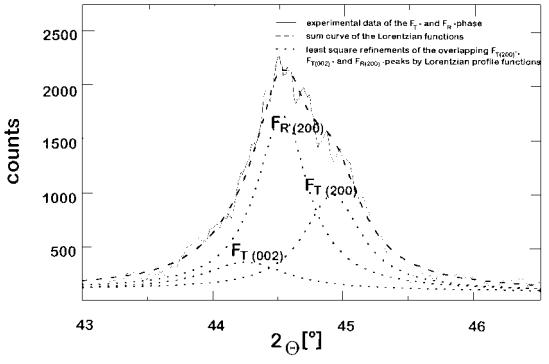

Fig. 4. X-ray diffraction pattern of a undoped PZT solid solution with a Zr/Ti-ratio of 53/47 and a least square refinement with Lorentzian profile functions of the overlapping $F_{T(002)}$-, $F_{T(200)}$- and $F_{R(200)}$-peaks.

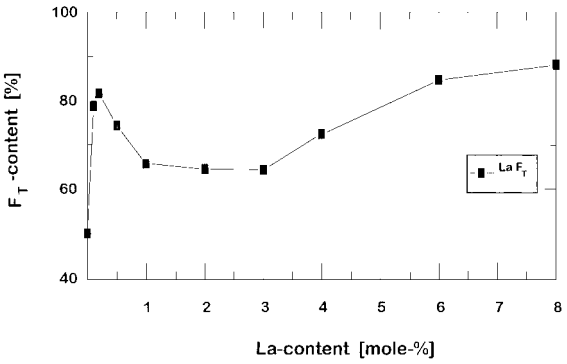

Fig. 6. Influence of La-content on the F_R/F_T-ratio of stoichiometric PZT solid solutions (53/47).

tetragonal modification was calculated using the following equation:

$$V_{uc} = a^2 \cdot c \tag{3}$$

In comparison to undoped samples the c/a-ratio as well as the V_{uc} starts to increase with La-doping. It could be observed that the c/a-ratio reaches its maximum of 2.4% for La-concentrations of 0.5 mole-%. Increasing amounts of additives lead to a continuous decrease of tetragonality to 1.013 for 8 mole-% La-containing samples which is 1% smaller in comparison to undoped PZT (Fig. 7).

A similar behavior could be observed for the V_{uc} of the F_T-phase. In comparison to undoped samples an increase of the V_{uc} could be found for La-concentrations < 1 mole-% whereas higher La-contents lead to a continuous decrease (Fig. 7). The maximum V_{uc} was 67.52 A^3 for the 0.1 and 0.2 mole-% La-containing samples which means an increase of 0.07% in comparison to undoped samples (Table 1).

Further X-ray diffraction investigations were related to the influence of La-content on the Curie-temperature (T_C). The measurements were performed on undoped and doped samples in the temperature range of 30–400°C with a Guinier diffractometer. Figure 8 shows as an example a temperature dependent phase transition of the F_T- and F_R-modification in the paraelectric P_C-modification in the angle range of $43° \leq 2\Theta \leq 46°$ for a 1 mole-% La-containing sample. The temperature difference between each diffraction pattern is 15°C and the detected phase transition occurred at 362°C. Below the corresponding T_C both the F_T-phase and the F_R-phase are stable. Rising the temperature above T_C results in a phase transition of the F_T- and F_R-phase into the P_C-phase which could be seen clearly by the disappearance of the overlapping $F_{T(200)}$-, $F_{T(002)}$- and $F_{R(200)}$-peaks and the detection of the $P_{C(200)}$ (Fig. 8). The reversible and continuous nature of the phase transition is demonstrated in Fig. 9 for a 4 mole-% La-containing sample revealing a phase transition at 270°C (±15°C). However, due to the limited resolution of the diffraction patterns it was not possible to detect a possible hysteresis during the heating and/or cooling process (Table 2).

Similar to the behavior of the tetragonality and V_{uc}, the Curie-temperature for samples with low additive contents (<1 mole-% La) was higher than for undoped samples. For La-concentrations of 0.5 and

Table 1. c/a-ratios and volume of the unit cells of La-containing stoichiometric PZT

Additive content [mole-%]	La a_T [Å]	La c_T [Å]	La a_R [Å]	La c_T/a_T	V_{uc} [A^3]
0	4.041	4.132	4.077	1.023	67.47
0.1	4.041	4.135	4.081	1.023	67.52
0.2	4.041	4.135	4.080	1.023	67.52
0.5	4.040	4.136	4.081	1.024	67.51
1	4.040	4.133	4.085	1.023	67.46
2	4.043	4.125	4.086	1.020	67.43
3	4.045	4.120	4.086	1.019	67.41
4	4.044	4.113	4.083	1.017	67.26
6	4.046	4.105	4.079	1.015	67.20
8	4.042	4.096	4.068	1.013	66.92

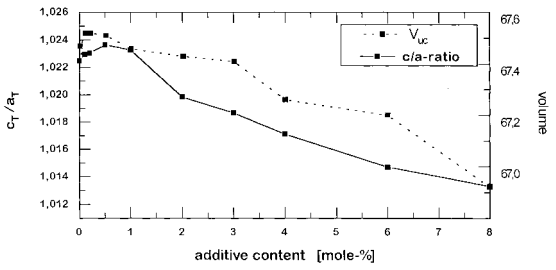

Fig. 7. c/a-ratio and volume of the unit cells of undoped and La-containing samples.

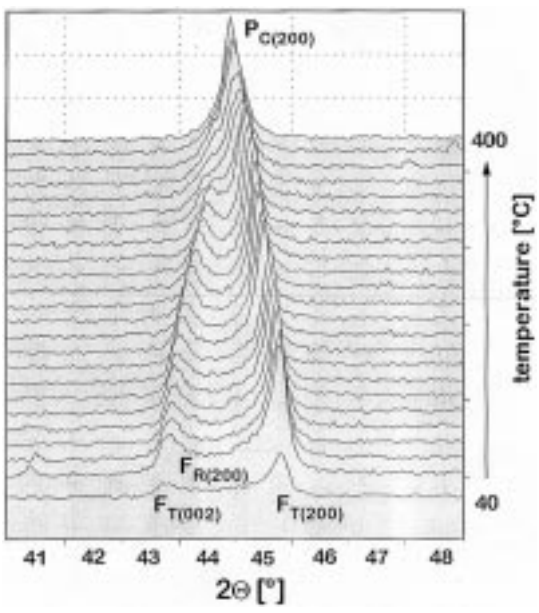

Fig. 8. X-ray diffraction patterns of a temperature dependent phase transition from F_T and F_R in P_C at 362°C.

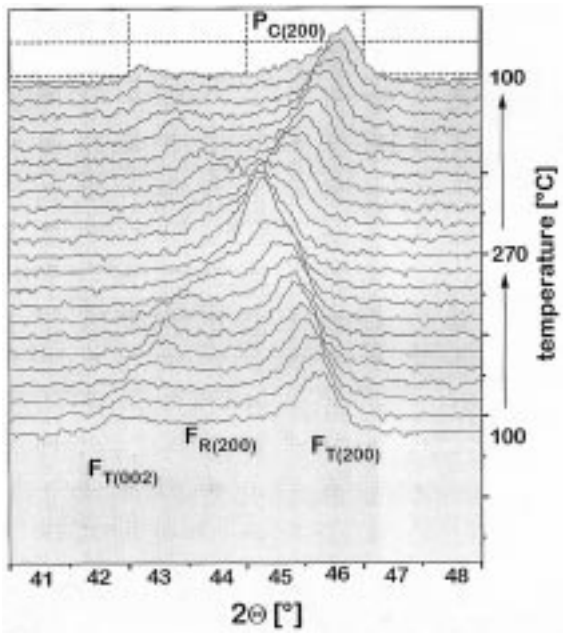

Fig. 9. X-ray diffraction patterns of a reversible phase transition of a 4 mole-% La-containing PZT ceramic revealing the phase transition at 270°C.

1.0 mole-% the observed T_C was 380 and 375°C, respectively whereas a continuous decrease could be observed for La-concentrations > 1 mole-% (Fig. 10).

3.3. Electromechanical Properties

Figure 11 shows the relative dielectric constant ε_r for undoped and La-doped PZT with and without PbO excess (poled and unpoled) after sintering at 1200°C for 2 h. The stoichiometric unpoled and poled samples show always a higher ε_r than the PbO excess ones (Table 3). In general it could be observed that the ε_r increase with increasing additive content and starts to decrease for La-concentrations >6 mole-%. A comparison of doped unpoled and poled samples clearly shows higher ε_r values for the poled PZT (ε_r^p) ceramics which could be observed

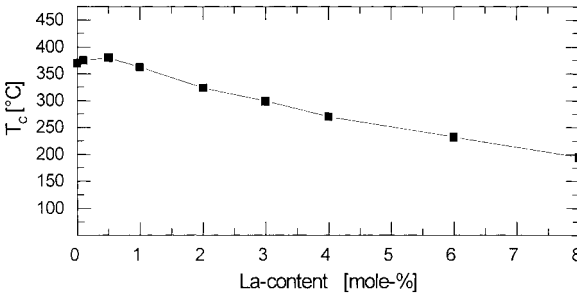

Fig. 10. Influence of the La-content on the Curie-temperature.

independent of the PbO content (except the 0.2 and 0.5 mole-% La-containing stoichiometric and PbO excess samples). However, for the undoped samples the unpoled ε_r (ε_r^{un}) were higher than the ε_n^pones (Table 3). The highest ε_r of the poled samples could be detected for 4 and 6 mole-% La-concentrations (1529 and 1558, respectively) whereas the unpoled samples show ε_r values of 1337 and 1410 for the same additive concentrations.

The coupling factor always revealed higher k_p for the stoichiometric samples in comparison to the PbO excess containing samples. The highest values were measured for 1 and 2 mole-% La-content (0.67) whereas samples containing the same additive concentration but PbO excess only showed a k_p of 0.57 and 0.62, respectively (Fig. 12). Stoichiometric samples as well as the PbO excess containing samples show a decrease of k_p with La-contents > 2 mole-% (Table 4).

Figure 13 shows the influence of PbO and the additive content on the T_C and the broadening of the peak of the dielectric constant. Obviously, the relative dielectric constant decreases significantly with high La-concentrations and reveals approximately 28,000 for samples with 2 mole-% La-content in comparison to 10,500 for samples containing 6 mole-% La. Simultaneously, the broadening of the peak increase for the higher doped samples. However, no significant influence on the T_C could be observed by sintering with an initial PbO excess (Fig. 13, Table 4).

Table 2. Influence of the La-concentration on the Curie-temperature

Additive content [mole-% La]	0	0.1	0.5	1	2	3	4	6	8
Zr/Ti	53/47	33/47	53/47	53/47	53/47	53/47	53/47	53/47	53/47
T_c [°C]	370	375	380	362	324	299	270	232	195

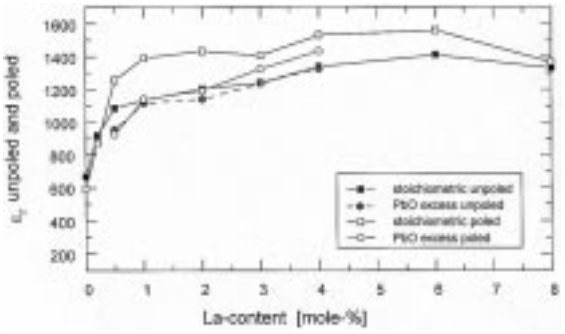

Fig. 11. Relative dielectric constant of poled and unpoled stoichiometric and PbO excess containing PZT.

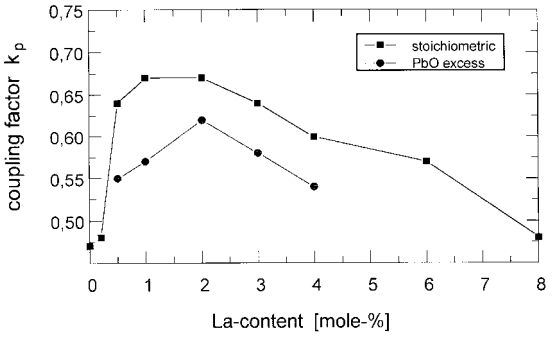

Fig. 12. Influence of La-content and PbO excess on the coupling factor k_p.

4. Discussion

4.1. Microstructure and X-ray Diffraction Analyses

The relative density reveals a higher porosity for samples containing low La additions (0.1 and 0.2 mole-%) compared to undoped or ≥ 0.5 mole-% containing ones. This phenomenon can be explained in terms of vacancy concentrations, which control the volume diffusion during densification. In thermodynamic equilibrium a certain number of Pb-vacancies exist in undoped materials; impurities in the raw materials as well as the pick-up of impurities during powder processing will further increase these ''equilibrium'' vacancy concentration. The Pb-vacancy concentrations in undoped PZT is high enough to obtain the observed high densification rate [20] with a resulting final relative density of 95.5% (Fig. 1). For specimens with low additive contents the number of vacancies will be partly compensated by the additive. Therefore the volume diffusion decreases and a lower relative density results (approximately 88%). The observed microstructural development is in good agreement with the results obtained from the X-ray diffraction analyses. It could be stated that the F_T-phase content was higher for samples containing lower La-concentrations of 0.1 to 0.5 mole-% compared to samples with additive contents of 1 to 3 mole-% La. Furthermore the lower doped samples reveal a higher c/a-ratio, V_{uc} and T_C than the undoped and higher doped ones. This behavior can also be attributed to the decrease in vacancy concentration which finally causes a stabilization of the perovskite structure. Higher additive contents (≥ 0.5 mole-% La) will create a significant amount of Pb-vacancies in order to achieve the electroneutrality condition and the volume diffusion and corresponding final densities $> 98\%$ are enhanced. Consequently, the structure is highly disturbed leading to the observed lower c/a-ratios, V_{uc} and Curie-temperatures. From crystal chemistry

Table 3. Dielectric constants of poled and unpoled La-containing and undoped PZT

	Stoichiometric			3 mole-% PbO excess		
La-content mole-%	ε_r^{un}	ε_r^{p}	$\varepsilon_r^{p} - \varepsilon_r^{un}$	ε_r^{un}	ε_r^{p}	$\varepsilon_r^{p-un}_{r}$
0 (Zr/Ti 53/47)	666	589	77	840	637	203
0.2	918	871	47	—	—	—
0.5	1086	1256	170	955	925	30
1	1134	1390	256	1118	1140	22
2	1203	1432	229	1141	1191	50
3	1238	1405	167	1236	1324	88
4	1337	1529	192	1327	1433	106
6	1410	1558	148	—	—	—
8	1330	1366	36	—	—	—

Table 4. Coupling factors and T_C as a function of La-content and PbO excess

La-content [mole-%]	Stoichiometric		3 mole-% PbO excess	
	T_C	k_p	T_C	k_p
0 (Zr/Ti 53/47)	378	0.47	—	—
0.2	374	0.48	—	—
0.5	365	0.64	367	0.55
1	358	0.67	356	0.57
2	335	0.67	320	0.62
3	315	0.64	311	0.58
4	295	0.6	304	0.54
6	248	0.57	—	—
8	208	0.48	—	—

a ferroelectric tetragonal PZT-structure consists of partially covalent bonded Ti(Zr)—O chains which form ordered dipoles oriented in one of the three axes. Additionally Pb^{2+} coordinates with four O^{2-} ions [21] and the oxygen atoms are more displaced from their original position in the cubic lattice. Simultaneously the polarization increases because of the additional contribution of the PbO dipoles and the polarization aligns with the ⟨001⟩-direction. In the rhombohedral modification the Pb^{2+} coordinates with three oxygen atoms leading to minor significance of the Ti(Zr)—O chains for the ferroelectricity as a result of the reduced titanium content. The polarization aligns with the ⟨111⟩-direction in which alternating TiO_3 and PbO_3 dipoles are formed [21]. An addition of La creates not only PbO-vacancies, but substitutes also Pb-ions and La—O bondings will partially replace Pb—O bondings. Due to the smaller electronegativity of the La^{3+}-ions in comparison to the Pb^{2+}-ions which is 1.1 and 2.33, respectively [22], the oxygen atoms are less

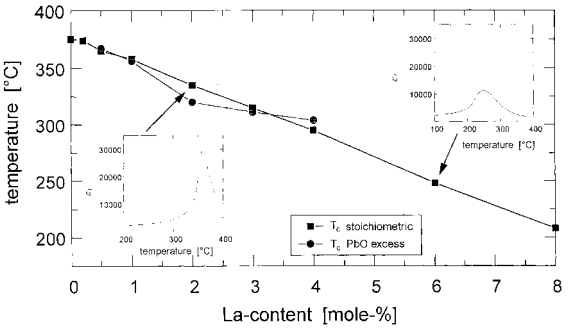

Fig. 13. Influence of La-content and PbO excess on the T_C and the width of the peak of the dielectric constant.

displaced and the contribution of the LaO dipoles on the polarizability is smaller. As a consequence, the tetragonality and V_{uc} decrease with increasing La-content (≥ 0.5 mole-%) as shown by X-ray diffraction measurements.

The additive dependency of the grain size shows the inverse tendency of the relative density plot. The grain size reveals a maximum for samples with 0.2 mole-% La-additions (Fig. 2). These maximum is attributed to a higher ratio of the grain growth rate to the densification rate for samples with small additive contents. Grain growth occurs only by surface diffusion and evaporation/condensation. Even if we assume that both mechanisms will not be changed significantly within the investigated compositions, a reduction of the lattice diffusion rate (main densification mechanism) due to the vacancy compensation will cause an increase of the ratio of grain growth rate over densification rate and explains the maximum in grain size. The reduced grain size for the additive-rich compositions is attributed to chemical inhomogeneities within the PZT grains as pointed out by Hammer and Hoffmann [20].

4.2. Microstructure and Electromechanical Properties

With an increase in chemical inhomogeneities and porosities, the electromechanical properties like dielectric constant and coupling factor will decrease. This behavior could be confirmed for low additive containing samples (0.1 and 0.2 mole-% La) which reveal higher porosities (approximatley 12%) (Fig. 1, Fig. 11 and Fig. 12) as well as for high additive containing samples (≥ 4 mole-%) which reveal a secondary phase [4,20] and a ''hole like'' structure due to chemical inhomogeneities within the PZT grains [4,20]. The higher dielectric constant for high additive containing samples can be explained by the higher tetragonal phase content due to the shift of the MPB in direction to Zr-rich compositions. The shift of the MPB superimpose the chemical inhomogeneities which leads in general to a decrease of ε_r. The observed ε_r-values are in good agreement with the results measured by Carl and Härdtl [12] and Takahashi [23].

The worst electromechanical properties of PbO excess containing samples (Fig. 11 and Fig. 12) are related to an amorphous PbO-rich secondary phase. This secondary phase is formed in accordance to the

ternary phase diagram of PbO-ZrO_2-TiO_2 [24] and was detected by several authors [4,25–27] in PZT ceramics with an initial PbO excess. Of course, the higher ε_r for higher additive contents compared to the undoped and low additive containing ones (0.2 mole-% La) has also been attributed to a higher domain wall motion due to a higher Pb-vacancy concentration [2,15,21].

A good correlation between the chemical inhomogeneities and the resulting lower dielectric properties can be given by temperature depending measurements of the dielectric constant (Fig. 13). It could be clearly seen that a higher doped sample (6 mole-% La) reveal a much lower ε_r at the Curie-temperature than a lower doped sample (2 mole-% La). Additionally the broadening of the peak of the dielectric constant for higher La-concentrations which could be described as a ''relaxor type'' behavior indicates different Curie-temperatures for different areas of chemically inhomogeneous PZT grains.

5. Summary

From the present results a strong relationship could be deduced among the densification behavior, the microstructural development, the observed X-ray diffraction analyses, and the electromechanical properties. It has been shown that the influence of the sintering behavior of PZT ceramics containing different dopant concentrations is strongly related to the measured c/a-ratio, V_{uc} and T_C. This behavior could be explained in terms of crystal and defect chemistry and it fits well with the measured porosities and grain sizes. Furthermore it was possible to relate the electromechanical data to the observed microstructure.

Acknowledgment

The authors would like to thank Dr. A. Endriss who conducted some of the X-ray diffraction measurements, and Dr. Lubitz and Dr. Kempter from Siemens AG, München for the measurement of the electromechanical properties. The authors also gratefully acknowledge the DFG for the financial support under contract No. Ho 1156/3-1.

Notes

1. PbO Analytical pure: Merck KGaA, Darmstadt, Germany.
2. ZrO_2 E101: MEL-Chemicals, Manchester, UK.
3. TiO_2 Bayertitan A-Z (Anatas): Bayer AG, Duisburg, Germany.
4. La_2-O_3 $>$ 99.9%: Ventron, Karlsruhe, Germany.

References

1. B. Jaffe, R.S. Roth, and S. Marzullo, *J. Appl. Phys.*, **25**, 809 (1954).
2. Y. Xu, *Ferroelectric Materials and Their Applications,* Elsevier Sci. Pub., Amsterdam, Netherlands, 1991).
3. A. Endriss, Ph.D. Thesis, University of Tuebingen, Germany (1995).
4. M. Hammer, Ph.D. Thesis, University of Karlsruhe, Germany (1996).
5. M. Hammer, C. Monty, A. Endriss, and M.J. Hoffmann, *J. Am. Ceram. Soc. 81* (3), 721–724 (1998).
6. H. Thomann, *Adv. Mater.*, **2**(10), 458–463 (1990).
7. W. Heywang und R. Schöfer, *Z. Angw. Phys.*, **20**, 10–15 (1965).
8. W. Wersing, G. Zorn, K. Lubitz, and J. Mohaupt, *Jpn. J. Appl. Phys.*, **24**, 724–726 (1985) Supplement 24- 2.
9. F. Kulcsar, *J. Am. Ceram. Soc.*, **42**, 343–349 (1959).
10. G.H. Haertling, *Am. Ceram. Soc. Bull.*, **43**(12), 113–118 (1964).
11. B. Jaffe, W.R. Cook, and H. Jaffe, in *Piezoelectric Ceramics*. Academic Press, London and New York (1971).
12. K. Carl and K.H. Härdtl, *Ber. Deutsch. Keram. Ges.*, **47**, 687–691 (1970).
13. G.H. Haertling and C.E. Land, *J. Am. Ceram. Soc.*, **54**, 1–11 (1971).
14. W. Rossner, Ph.D. Thesis, University of Erlangen, Germany (1985).
15. R.B. Atkin and R.M. Fulrath, *J. Am. Ceram. Soc.*, **54**, 265– 270 (1971).
16. J. Ihringer and K. Roettger, *J. Phys. D: Appl. Phys.*, **26**, A32–A34 (1993).
17. K. Roettger, Ph.D. Thesis, University of Tuebingen, Germany (1995).
18. K. Metha and A.V. Virkar, *J. Am. Ceram. Soc.*, **73**, 567–574 (1990).
19. S. Cheng and K. Lloyd, *J. Am. Ceram. Soc.*, **75**, 2293–2296 (1992).
20. M. Hammer and M.J. Hoffmann, *J. Am. Ceram. Soc.* (to be published 1998).
21. W. Heywang and H. Thomann, *Ann. Rev. Mater. Sci.*, **14**, 27–47 (1984).
22. L. Pauling, *The Nature of the Chemical Bond*, Cornell University Press (1960).
23. S. Takahashi, *Ferroelectrics*, **41**, 143–156 (1982).
24. T. Ikeda and S. Fushimi, *J. Am. Ceram. Soc.*, **30**, 129–132 (1967).
25. S.-S. Chiang, M. Nishioka, R.M. Fulrath, and J.A. Pask, *J. Am. Ceram. Bull.*, **60**, 484–489 (1981).
26. E.K.W. Goo, R.K. Mishra, and G. Thomas, *J. Am. Ceram. Soc.*, **64**, 517–519 (1979).
27. C.- C. Hsueh and M.L. Mecartney, *J. Mat. Sci. Lett.*, **8**, 1209–1215 (1989).